



**HAL**  
open science

## Role of the resonator geometry on the pressure spectrum of reed conical instruments

Jean Kergomard, Philippe Guillemain, Patrick Sanchez, Christophe Vergez,  
Jean-Pierre Dalmont, Bruno Gazengel, Sami Karkar

► **To cite this version:**

Jean Kergomard, Philippe Guillemain, Patrick Sanchez, Christophe Vergez, Jean-Pierre Dalmont, et al.. Role of the resonator geometry on the pressure spectrum of reed conical instruments. 2019. hal-01865994v2

**HAL Id: hal-01865994**

**<https://hal.science/hal-01865994v2>**

Preprint submitted on 1 Feb 2019

**HAL** is a multi-disciplinary open access archive for the deposit and dissemination of scientific research documents, whether they are published or not. The documents may come from teaching and research institutions in France or abroad, or from public or private research centers.

L'archive ouverte pluridisciplinaire **HAL**, est destinée au dépôt et à la diffusion de documents scientifiques de niveau recherche, publiés ou non, émanant des établissements d'enseignement et de recherche français ou étrangers, des laboratoires publics ou privés.

# Role of the resonator geometry on the pressure spectrum of reed conical instruments

Jean Kergomard, Philippe Guillemain, Patrick Sanchez, Christophe Vergez<sup>1</sup>,  
Jean-Pierre Dalmont, Bruno Gazengel<sup>2</sup>, Sami Karkar<sup>3</sup>,

<sup>1</sup> Aix Marseille Univ, CNRS, Centrale Marseille, LMA,  
UMR 7031, Marseille, France

<sup>2</sup> LUNAM Université, Université du Maine, Unité Mixte de Recherche CNRS 6613,  
Avenue Olivier Messiaen, 72085 Le Mans Cedex 9, France

<sup>3</sup> Univ Lyon, Ecole Centrale de Lyon, ENISE, ENTPE, CNRS,  
Laboratoire de Tribologie et Dynamique des Systèmes LTDS,  
UMR5513, F-69134, ECULLY, France

## 1 Summary

Spectra of musical instruments exhibit formants or anti-formants which are important characteristics of the sounds produced. In the present paper, it is shown that anti-formants exist in the spectrum of the mouthpiece pressure of saxophones. Their frequencies are not far but slightly higher than the natural frequencies of the truncated part of the cone. To determine these frequencies, a first step is the numerical determination of the playing frequency by using a simple oscillation model. An analytical analysis exhibits the role of the inharmonicity due to the cone truncation and the mouthpiece. A second step is the study of the input impedance values at the harmonics of the playing frequency. As a result, the consideration of the playing frequency for each note explains why the anti-formants are wider than those resulting from a Helmholtz motion observed for a bowed string. Finally numerical results for the mouthpiece spectrum are compared to experiments for three saxophones (soprano, alto and baritone). It is shown that when scaled by the length of the missing cone, the anti-formant frequencies in the mouthpiece are very similar for the three instruments. The frequencies given by the model are close to the natural frequencies of the missing cone length, but slightly higher. Finally, the numerical computation shows that anti-formants and formants might be found in the radiated pressure.

## 1 Introduction

The auditory recognition of musical instruments is a rather intricate issue. It is generally admitted that the existence of formants is an important element that contributes to the identification of an instrument. A formant (resp. an anti-formant) can be defined

as a frequency band reinforced (resp. attenuated) whatever the played note. Formants are in general regarded as an important characteristic of the tone colour (or of the vowels in speech). It needs to be distinguished from other timbre characteristics, such as the weakness of harmonics of a given rank (e.g., the even harmonics in the clarinet sound). The statement of the problem is ancient [4, 5]. Smith and Mercer [4] found formants produced by conical instruments similar to saxophones. Benade [2] wrote: “There is in fact almost no simple formant behavior to be recognized in the sound production of wind instruments”. However several authors observed that the spectrum of the acoustic pressure in the reed of a bassoon [1] or in the mouthpiece of a saxophone [2, 3] is close to the function  $\sin(nq)/nq$ , where  $n$  is the harmonic number and  $q$  can be determined experimentally.

This implies that anti-formants can appear around frequencies satisfying  $\sin(nq) = 0$ . If formants (or anti-formants) exist, a consequence of the above mentioned definition is that their frequencies cannot depend on the length of the tube for a given note. Conversely they depend either on other geometrical parameters (length of the missing cone, input radius, apex angle of the truncated cone, dimensions of the mouthpiece, geometry of the toneholes) or on the excitation parameters.

The simplest model, based upon the analogy with bowed string instruments, was studied by many authors [6, 7, 8, 9, 10, 11, 12], and a result is the wave-shape approximation of the mouthpiece pressure by a rectangle signal, i.e., the waveshape of the ideal Helmholtz motion. Formerly, some authors explained that an approximation of the natural frequency of reed conical instruments is equal to that of an “open-open” cylinder whose length is the length of the truncated cone extended to its apex [13, 14, 15]. Because

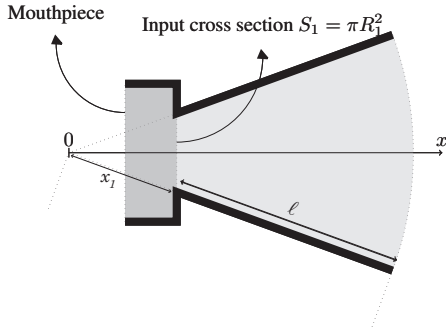


Figure 1: Notations for the geometrical parameters. For a soprano saxophone, the length of the missing part of the cone is approximately  $x_1=0.126$  m. Typical values of the coefficient  $\beta$  are included in the interval  $[0.13, 0.3]$ .

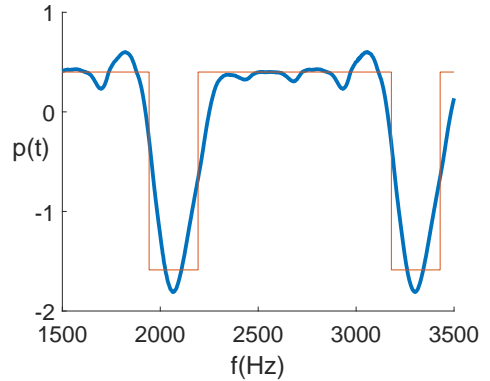


Figure 2: Example of waveshape for a soprano saxophone ( $x_1 = 0.126$ m and  $\ell = 0.55$ m) for the excitation parameters  $\gamma = 0.4$ ,  $\zeta = 0.65$  (see Sect. 3.1). Thick line: RTC model; thin line: ideal Helmholtz motion model.

72 the length of the missing cone does not vary with the  
73 note, a consequence of the analogy is that the dura-  
74 tion of the negative pressure episode is common to  
75 all notes. Another consequence is the existence of  
76 anti-formants close to the natural frequencies of the  
77 missing part of the truncated cone (which is denoted  
78  $x_1$  in the present paper, see Fig. 1 for the notations).

79 The analogy with the Helmholtz motion of bowed  
80 strings leads to the result that in the function  
81  $\sin(nq)/nq$ ,  $q \simeq \pi\beta$ , where  $\beta$  is the ratio of the short  
82 length of the string to its total length. For a trun-  
83 cated cone,  $\beta$  is the ratio of the length of the missing  
84 cone  $x_1$  to the total length  $x_2 = \ell + x_1$  :

$$\beta = \frac{x_1}{x_1 + \ell} = \frac{x_1}{x_2} = \frac{R_1}{R_2} \quad (1)$$

85  $R_1$  and  $R_2$  are the radii at abscissae  $x_1$  and  $x_2$ , re-  
86 spectively.

87 It is still the only model that yields analytical ex-  
88 pressions for the sound produced, and therefore it is  
89 used as a reference for the present study. In a pa-  
90 per written by some of the present authors, it was  
91 shown that a simple numerical model can largely im-  
92 prove the model of the Helmholtz motion [16]. We call  
93 it the ‘‘Reed-Truncated-Cone’’ model (RTC model).  
94 The difference between the two models lies in the res-  
95 onator model. Example of waveshapes obtained with  
96 the two models are shown in Fig. 2. Using the RTC  
97 model for the present investigation on the spectrum,  
98 the paper aims at further understanding of the exis-  
99 tence of formants or anti-formants in the mouthpiece  
100 pressure spectrum, and, to some extent, of the exter-  
101 nal pressure. The computation is done ab initio in the  
102 time domain.

103 The study is limited to the first register, which re-  
104 sembles the Helmholtz motion (periodic regime, one  
105 positive pressure and one negative pressure episodes).  
106 The RTC model is based upon the observation that  
107 in practice the mouthpiece volume is approximately  
108 equal to that of the missing cone [17], entailing a weak

109 inharmonicity for the lower notes. The resonator is a  
110 truncated cone, of length  $\ell$ , with a pure lumped com-  
111 pliance at its input (that of the air in the mouthpiece  
112 volume). This is a simplification, because in some  
113 instruments, such as the oboe, the cone of the res-  
114 onator can be more complicated, with two different  
115 tapers, entailing a further reduction of inharmonicity  
116 [18]. The double taper is not considered here, be-  
117 cause the waveform of the internal pressure given by  
118 the RTC model seems to compare well enough with  
119 experimental waveforms [16].

120 The effects of wall losses and radiation are ignored.  
121 The model of toneholes is extremely simplified: for a  
122 given fingering with a given number of toneholes, the  
123 resonator is assumed to be equivalent to a truncated  
124 cone of equivalent length  $\ell$ . Therefore, for a given  
125 note, two parameters are sufficient, the length  $\ell$  and  
126 the radius ratio  $R_2/R_1$  (actually, without losses, it is  
127 not necessary to define the values of the two radii,  
128 or the apex angle). Therefore, according to the hy-  
129 potheses adopted in the RTC model, the length of  
130 the missing cone is expected to be predominant in the  
131 dependence of the frequencies of formants and anti-  
132 formants.

133 As an intermediate step, the paper attempts to de-  
134 termine more precise values for the first playing fre-  
135 quency, because it has an influence on the spectrum,  
136 as discussed later. This influence entails the depen-  
137 dence of the pressure spectra on the fingering, i.e., on  
138 the length  $\ell$ , and the enlargement of the formants.

139 In Sect. 2 the RTC model is presented for the res-  
140 onator, with the calculation of the transfer functions  
141 of the resonator (between input and output quanti-  
142 ties). Sect. 3 recalls some known results about the  
143 ‘‘cylindrical saxophone’’ model, which is similar to  
144 that of an ideal bowed string, and gives the classi-  
145 cal solution of the Helmholtz motion. The paradox  
146 of the analogy between a conical instrument and a

147 cylindrical saxophone is discussed.

148 Then, in Sec. 4, it is shown how the playing fre-  
 149 quencies for a truncated cone with mouthpiece differ  
 150 from those corresponding to the ideal Helmholtz mo-  
 151 tion, because they depend on the excitation param-  
 152 eters, and on the note.

153 In Sec. 5 the zeros of the transfer functions are in-  
 154 vestigated with their dependence on the playing fre-  
 155 quencies.

156 In Section 6, thanks to the results of numerical com-  
 157 putations obtained with the RTC model [16] of the  
 158 sound production, the frequencies of the minima of  
 159 the sampled input impedance are compared to those  
 160 of the mouthpiece pressure, and the existence of for-  
 161 mants and anti-formants is discussed in both the in-  
 162 ternal pressure and the external one.

163 In Section 7 experimental results are presented, and  
 164 compared to the numerical results.

## 165 2 Basic model of the resonator

### 166 2.1 Resonator model of the RTC.

167 A truncated cone is considered (see Fig. 1), provided  
 168 with a mouthpiece of volume equal to the volume of  
 169 the missing cone:  $V = x_1 S_1/3$ . The mouthpiece is  
 170 assumed to be small with respect to the wavelength.  
 171 The shunt acoustic compliance of the mouthpiece is  
 172  $V/\rho c^2$ . The inertia of the air within the mouthpiece  
 173 (i.e. the series acoustic mass), is ignored, because the  
 174 sound production by reed instruments occurs at fre-  
 175 quencies close to impedance maxima (this is discussed  
 176 in Ref. [16]). At abscissae  $x_1$  and  $x_2$ , the cross-section  
 177 areas are  $S_1$  and  $S_2$ , respectively. No resonator losses  
 178 are considered, and the output impedance of the cone  
 179 is assumed to be zero. This implies that the radiation  
 180 reactance is zero too: it could be taken into account  
 181 by a slight modification of the length of the truncated  
 182 cone. In the frequency domain, the solution of the  
 183 acoustic equations in the conical tube can be written  
 184 as the sum of two spherical, travelling pressure waves  
 185  $P^\pm(x)$  (see e.g. [19]):

$$P(x) = P^+(x) + P^-(x); \quad (2)$$

$$U(x) = \frac{S(x)}{\rho c} \left( P^+(x) - P^-(x) + \frac{P(x)}{jkx} \right) \quad (3)$$

$$P^\pm = a^\pm \exp(\mp jkx)/x. \quad (4)$$

186  $P(x)$  is the pressure and  $U(x)$  is the flow rate.  $k =$   
 187  $2\pi f/c$  is the wavenumber,  $f$  is the frequency,  $c$  the  
 188 speed of sound,  $\rho$  the air density. Standard transfer  
 189 matrices for the lumped compliance and the truncated  
 190 cone are used for this model in the frequency domain.  
 191 Because the pressure  $P_2$  at the output is zero, the two  
 192 following transfer functions between the mouthpiece  
 193 input quantities (pressure  $P$  and flow rate  $U$ ) and the

output flow rate  $U_2$  are found: 194

$$P = \frac{j\rho c}{\pi R_1 R_2} \sin(k\ell) U_2, \quad (5)$$

$$U = \frac{R_1}{R_2} \{ \cos(k\ell) + \sin(k\ell)/(kx_1) - \sin(k\ell)kx_1/3 \} U_2 \quad (6)$$

195 These transfer functions have zeros, but no poles.  
 196 At the frequencies of the zeros, because  $U_2$  is finite,  
 197 the input quantities  $P$  and  $U$  vanish. The external  
 198 pressure can be derived from the output flow rate  
 199  $U_2$ , which at low frequencies can be regarded as a  
 200 monopole source. Omitting the delay, the low fre-  
 201 quency relationship between the external pressure at  
 202 distance  $d$  and the output flow rate is the following:

$$P_{ext} = j\omega\rho U_2 \frac{1}{4\pi d}. \quad (7)$$

203  $\omega$  is the angular frequency. For our purpose, we have  
 204 interest in the physical quantities  $P$ ,  $U$  and  $U_2$ , which  
 205 depend on the excitation, as well as the extrema of  
 206 the two transfer functions, which depend on the res-  
 207 onator only. The zeros of the transfer functions for  
 208 the pressure and flow rate (Eqs. (5) and (6)) are the  
 209 zeros and poles, respectively, of the input impedance:

$$Z = \frac{\rho c}{S_1} \frac{j \sin(k\ell)}{\cos(k\ell) + \sin(k\ell)/(kx_1) - \sin(k\ell)kx_1/3}. \quad (8)$$

### 210 2.2 Comparison with the ‘‘cylindrical 211 saxophone’’ model

212 A further approximation of the RTC model is the  
 213 classical cylindrical saxophone model. The function  
 214  $1/x - x/3$  is identified with the expansion of the func-  
 215 tion  $\cot(x)$ . The transfer function equation (6) is un-  
 216 changed, and, under the following condition,

$$kx_1 = 2\pi x_1/\lambda \ll 1, \quad (9)$$

217 where  $\lambda$  is the wavelength, Eq. (6) becomes:

$$U = \frac{R_1}{R_2} [\cos(k\ell) + \sin(k\ell) \cot(kx_1)] U_2. \quad (10)$$

218 The input impedance becomes:

$$Z = \frac{j\rho c}{S_1} \frac{\sin(k\ell) \sin(kx_1)}{\sin[k(\ell + x_1)]}. \quad (11)$$

219 This formula is equivalent to that of the admittance of  
 220 a string at the bow position. Therefore the Helmholtz  
 221 motion is a particular solution of the self-sustained  
 222 oscillation problem. We call this model ‘‘cylindrical  
 223 saxophone’’ model (however for a cylinder  $R_1 = R_2$ ,  
 224 while here the radii  $R_1$  and  $R_2$  are different). Com-  
 225 paring Eqs. (6) and (10), it can be noticed that in the  
 226 transformation, an infinity of poles have been added,  
 227 entailing different behaviours of the transfer functions  
 228 and input impedance.

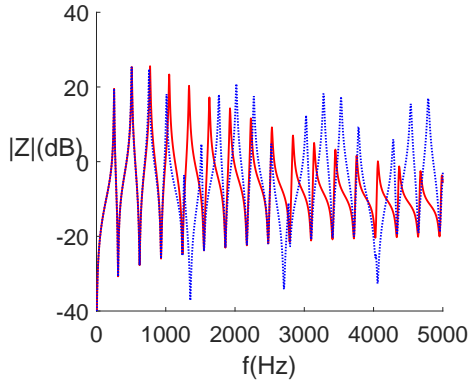


Figure 3: Example of input impedance modulus curves (dB defined by  $20\log(|ZS_1/\rho c|)$  for  $x_1 = 0.126\text{m}$  and  $\ell = 0.55\text{m}$ . Solid line (red online): RTC model; dotted line (blue online): approximation corresponding to the cylindrical saxophone model (ideal Helmholtz motion).

Formula (11) exhibits that there are two kinds of input impedance dips: i) the solutions of  $\sin(k\ell) = 0$ , which depend on the note; ii) the solutions of  $\sin(kx_1) = 0$ , which do not depend on the note. Fig. 3 shows an example of input impedance curve. For this figure, realistic visco-thermal losses (for an average cone radius) have been taken into account in Eq. (11). The two kinds of dips appear. We add three remarks:

1. The case shown in Fig. 3 corresponds to an irrational value of the parameter  $\beta$ . For rational values of  $\beta$ , the frequencies of the second kind of dips for the cylindrical saxophone can coincide with those of the truncated cone, but losses make the dips distinct.
2. The resonances of the cylindrical saxophone are perfectly harmonic (see the dotted lines in Fig. 3). The figure exhibits that this is not the case for the truncated cone with mouthpiece (solid line in Fig. 3). For the RTC model the second kind of minima disappears, according to Eq. (8). The comparison between the RTC model and the cylindrical saxophone model shows the effect of inharmonicity. It will be shown in Sections 4 and 5 that, as a consequence, minima close to dips of the cylindrical saxophone appear in the input impedance *at the harmonics of the playing frequency*. For these harmonics, we call the input impedance curve the sampled impedance (see [20]).
3. These minima are responsible for anti-formants of the input pressure, because their frequencies depend few of the note.

### 3 Oscillation model and the solution of the ideal Helmholtz motion

#### 3.1 Helmholtz motion

The complete oscillation model is now investigated for the cylindrical saxophone. For the exciter (mouth and reed), the model used was presented in Ref. [16]. The nonlinear characteristic is deduced from the model established by Wilson and Beavers [21]. Nevertheless no reed dynamics is considered. Two dimensionless parameters were defined by these authors: the mouth pressure  $\gamma$  and the reed opening  $\zeta$  at rest (in Ref. [21], the parameters are the same, with different notations). The model is based upon the stationary Bernoulli law and some hypotheses, with a localized non-linearity. With the approximation (11) for the impedance, analytical solutions exist for the oscillations, in particular the so-called Helmholtz motion [9], which is a rectangle signal.

Using the subscript  $H$  for the Helmholtz motion, the fundamental frequency is  $f_{H1} = c/2(\ell + x_1)$  (the wavelength is twice the total length of the cone). The frequency  $f_{Hn}$  of the  $n$ th harmonic is given by:

$$f_{Hn} = \frac{nc}{2(\ell + x_1)}. \quad (12)$$

The value of the signal during the longer episode is  $\gamma$  (when the reed does not close the mouthpiece), while the value during the shorter episode is  $-(1 - \beta)\gamma/\beta$  (when the reed closes the mouthpiece, for the definition of  $\beta$ , see Eq. (1)). This case corresponds to the condition  $\gamma > \beta$ , which is often satisfied in practice at least for the lowest notes (see Ref. [9]), as well for the choice of parameters in the theoretical part of the present paper. The spectrum components of the input pressure  $p(t)$  are as follows:

$$P_n = -\gamma (-1)^n \frac{\sin X_n}{X_n} \quad (13)$$

$$X_n = 2\pi \frac{f_{Hn} x_1}{c} = k_{Hn} x_1 \quad (14)$$

$$= \frac{n\pi x_1}{\ell + x_1} = n\pi\beta. \quad (15)$$

Here, and in what follows, the pressure is dimensionless: all pressures in the resonator are divided by the reed closure pressure  $p_M$ , which is proportional to the reed stiffness. The waveshape and the relative pressure spectrum are independent of the excitation parameters. The flow rate  $u(t)$  at the input is constant, in order for the input average power per period to vanish. For frequencies  $f_m = mc/(2x_1)$ ,  $\sin X_m = \sin(m\pi) = 0$ : there is a zero in the pressure spectrum, under the condition that  $m/n = \beta$  is rational. If  $\beta$  is irrational, there is a minimum amplitude near the frequencies  $f_m$ . As a consequence, whatever the cone length  $\ell$ , there is an amplitude minimum around these frequencies, i.e., an anti-formant, and

309 these frequencies are the natural frequencies of the  
 310 length  $x_1$  of the missing cone.

311 Writing  $x_1 = (\ell + x_1) - \ell$ , Eq. (13) implies:

$$\begin{aligned} \sin X_n &= (-1)^n \sin(n\pi\ell/(\ell + x_1)) & (16) \\ &= (-1)^n \sin(k_{Hn}\ell), & (17) \end{aligned}$$

312 thus Eqs. (6) and (13) give the amplitude of the out-  
 313 put flow rate:

$$U_{2,n} = \frac{\gamma}{X_n} \frac{\pi R_1 R_2}{\rho c}. \quad (18)$$

314 There are no zeros in the spectrum of the output  
 315 flow rate. Eqs. (7, 18) show that the spectrum of the  
 316 external pressure  $P_{ext}$  is constant and the signal is a  
 317 Dirac comb. Neither formants nor anti-formants exist  
 318 in the radiated pressure  $P_{ext}$ .

### 319 3.2 Comparison of a cylindrical saxo- 320 phone with a truncated cone

321 The present study was motivated by a paradox pre-  
 322 sented in a conference paper by some authors of the  
 323 present article [23], and summarized hereafter.

324 For bassoon sounds, Gokhstein [7] showed both ex-  
 325 perimentally and theoretically that the duration of  
 326 reed closure is independent of the played note, i.e., of  
 327 the equivalent length of the resonator. This duration  
 328 is related to the round trip of a wave over a length  
 329 equal to that of the missing part of the cone  $x_1$ . The  
 330 corresponding frequency is the natural frequency of  
 331 this length  $c/(2x_1)$ . This seems to validate the anal-  
 332 ogy with the bowed string excited at a given length of  
 333 the bridge (or with the cylindrical saxophone, which  
 334 is also analogous to a kind of stepped cone [10]). This  
 335 was studied in several papers [8, 9, 10]. However the  
 336 analogy is known to be valid only if the length of the  
 337 missing cone is small compared with the wavelength  
 338 (see Condition (9)). This condition is not fulfilled for  
 339 the natural frequency of the missing part, which is  
 340 equal to the half of the corresponding wavelength.

341 Thanks to the bowed string analogy, useful conclu-  
 342 sions can be drawn concerning important features of  
 343 the sound production, such as oscillation regimes and  
 344 amplitudes. A priori accurate insight of the tone color  
 345 for higher frequencies, which do not fulfill the condi-  
 346 tion (9), cannot be expected. Nevertheless measured  
 347 spectra of the internal pressure of saxophones exhibit  
 348 minima [22] at frequencies corresponding roughly to  
 349 the harmonics of the fundamental frequency  $c/(2x_1)$ .  
 350 On the one hand this is an argument in favour of  
 351 the analogy with the Helmholtz motion, while on the  
 352 other hand this result is paradoxical because for these  
 353 frequencies, the condition (9) is not fulfilled. It will  
 354 be shown how inharmonicity of the resonator, which  
 355 exists neither in a perfect string nor in a cylindrical  
 356 saxophone, plays a major role in a real conical instru-  
 357 ment. In particular it implies that the playing fre-

quency differs from natural frequencies  $c/(2(x_1 + \ell))$   
 of the complete cone.

In order to make easier the comparison of the re-  
 sults for a truncated cone with those for the Helmholtz  
 motion, we define a quantity proportional to the ex-  
 ternal pressure (Eq. (7)) and inversely proportional  
 to the blowing pressure, i.e., to the square root of the  
 radiated power, as follows:

$$W = U_2 \frac{\rho c}{\pi R_1 R_2 \gamma} k x_1. \quad (19)$$

We call  $W$  the normalized output flow rate. For the  
 Helmholtz motion and the harmonics of the playing  
 frequency, which is our reference,  $|W|$  is unity (see  
 Eqs. (18) and (15)). For the truncated cone, we re-  
 define the transfer functions (5 and 6), as follows:

$$\begin{pmatrix} P \\ U \end{pmatrix} = \begin{pmatrix} F_p \\ F_u \end{pmatrix} W \quad (20)$$

with

$$F_p = \frac{j\gamma}{k x_1} \sin(k\ell), \quad (21)$$

$$F_u = \frac{S_1}{\rho c} \frac{\gamma}{k x_1} \{(\cos(k\ell) + \sin(k\ell))/(k x_1) - \sin(k\ell)k x_1/3\}. \quad (22)$$

## 4 Playing frequency of a conical instrument

The playing frequency is a compromise between the  
 different modes of the resonator and varies with the  
 excitation parameters (see especially [24, 25]). For a  
 truncated cone, the playing frequencies slightly differ  
 from the resonance frequencies of the cylindrical sax-  
 ophone, and the consequences for the pressure spec-  
 trum are significant. In the present section the values  
 of the playing frequency are studied. Then, in section  
 5 the dependence of the formants and anti-formants  
 on the playing frequency is investigated.

It is often considered that the playing frequen-  
 cies are very close to the natural frequencies of the  
 resonator. However several causes of discrepancies  
 between playing and natural frequencies were re-  
 cently investigated for reed cylindrical instruments  
 [26]. Among them there is the effect of inharmonicity  
 of the resonator for conical instruments, which are  
 truncated cones. The effect of the truncation is im-  
 portant, even if it is limited by a proper choice of the  
 mouthpiece dimensions. When the approximation of  
 the cylindrical saxophone is abandoned, the playing  
 frequencies differ from the natural frequencies of the  
 total length  $\ell + x_1$  (Eq. (12)).

### 4.1 Numerical estimation of the play- ing frequencies (RTC model)

Using the numerical RTC model, including the exci-  
 tation model and the resonator model corresponding

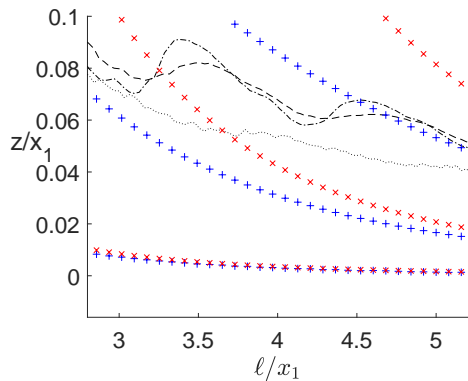


Figure 4: Length  $z$  ( $-z$  is the length correction) related to the playing frequency represented by the ratio  $\ell/x_1$  for several values of the length  $\ell$  of the truncated cone (simulation results). When  $\ell$  varies from 0.35 m to 0.67 m, the ratio  $\beta$  decreases from 0.26 to 0.16.  $x_1 = 0.126$ m. Thin, black lines: dotted ( $\gamma = \zeta = 0.4$ ), mixed ( $\gamma = 0.45$ ;  $\zeta = 0.85$ ), dashed ( $\gamma = 0.4$ ;  $\zeta = 0.65$ ). +++ -blue online) Formula (25), for one, two, three terms of the series (from bottom to top). xxx (red online) Formula (26), for one, two, three terms of the series (from bottom to top).

to Eq. (8), the playing frequency of the first periodic regime was determined. In order to calculate the playing frequency, we seek the number of samples between two changes in sign of the input pressure (when the pressure is negative and becomes positive). The typical number of samples for one period is larger than 1000. The relative error on the total equivalent length is less than 0.1%, and that on the length correction is less than 1%.

It is convenient to represent the shift between the playing frequency  $f_p$  and that of the ideal Helmholtz motion by a length correction, denoted  $-z$ , as follows :

$$k_p = \frac{2\pi f_p}{c} = \frac{\pi}{\ell + x_1 - z}. \quad (23)$$

$z = 0$  corresponds to the case where these two frequencies are equal. The thin lines in Fig. 4 show, for three pairs of  $(\gamma, \zeta)$ , that the length correction is negative, entailing that the playing frequency is higher than the first resonance frequency. The length  $z$  is significantly smaller than the length  $x_1$  of the missing cone, and consequently much smaller than the total length, whatever the value of the cone length  $\ell$ . However the comparison of the classical approximation of the resonance frequency  $c/2/(\ell + x_1)$  and the playing frequency shows that the difference between them is not negligible: 4% for  $\ell = 0.35$ m, i.e., 60 cents, and 1% for the lowest note ( $\ell = 0.67$  m), i.e., 15 cents.

For dimensions close to those of a soprano saxophone, the choice of 0.35m as the shortest value for the cone length is due to the difficulty for finding a periodic regime with the ab initio computation and

a short  $\ell$ . The playing frequencies are in the range [209Hz, 438Hz] for  $c = 340$  ms<sup>-1</sup>. The issue of the regime stability is complicated, and is out of the scope of the present paper (see [9, 12, 27]).

## 4.2 Analytical estimation of the playing frequencies

In order to understand the role of inharmonicity in the playing frequency, the influence of the second resonance frequency, which is higher than twice the first, and that of the third one, can be estimated in a quantitative way. For this purpose, the result due to Boutillon [28] is used, valid under the condition that the reed dynamics is ignored. With this condition, this is one of the equations of the Harmonic Balance Method (HBM, see for an explanation [19, p. 518]), therefore it does not need the computation of the transient. Considering that the length correction depends little on the excitation parameters, the spectrum of the input pressure is approximated by its value for the Helmholtz motion, and it is possible to find analytically an order of magnitude of the length correction. The “reactive power rule” leads to the equation to be solved for the unknown playing frequency, denoted  $\omega$ :

$$\sum_n n |P_n|^2 \text{Im}[Y(n\omega)] = 0. \quad (24)$$

$P_n$  is given by Eq. (13). In Appendix A, two approximate methods of calculation for the corresponding length correction  $-z$  are used. The first one gives the result:

$$z = \frac{\sum_n z_n n^2 \sin^2(n\pi\beta) / \text{Res}_n}{\sum_n n^2 \sin^2(n\pi\beta) / \text{Res}_n}, \quad (25)$$

where  $z_n$  is the length correction corresponding to the  $n$ th resonance frequency and  $\text{Res}_n$  the residue of this resonance in the formula (8) of the input impedance. If the lengths  $z_n$  were equal for all resonance frequencies (no inharmonicity), the correction for the playing frequency would be equal to them.

Fig. 4 compares the numerical results with those obtained using the two formulas (25) and (26, see hereafter). For the first one, the main features are the correct order of magnitude when more than one term are kept in Eq. (25), and the global decrease when the length  $\ell$  increases. The difference between the results with 1 and 2 terms exhibits the importance of the inharmonicity between the first two resonances, due to the truncation of the cone (the result limited to one term is nothing else than the length correction for the first resonance). It appears that the playing frequency obtained from the numerical computation lies between the results of Eq. (25) for 2 and 3 harmonics (i.e., for 2 and 3 terms of the series). The calculation with 4 terms gives bad results, as explained in



480 Appendix A, after Eq. (A10). It can be concluded  
 481 that the second and third harmonics play an impor-  
 482 tant role in the value of the playing frequency. More-  
 483 over, although the excitation is ignored in Eq. (25),  
 484 this calculation gives a qualitative agreement with the  
 485 complete computation of the oscillations.

486 The second method is an analytical approximation  
 487 of Eq. (25), which is satisfactory for one harmonic,  
 488 but for two and three harmonics, it is satisfactory only  
 489 for long length  $\ell$  ( $\ell \gg x_1$ ), i.e., when the resonance  
 490 frequencies are low. It gives the following approxima-  
 491 tion:

$$z \simeq x_1 \frac{\pi^4 \beta^4}{45} \frac{1 + 16 \cos^2(\pi\beta) + 9 [3 - 4 \sin^2(\pi\beta)]^2}{1 + \cos^2(\pi\beta) + [3 - 4 \sin^2(\pi\beta)]^2 / 9}. \quad (26)$$

492 The three terms of the numerator and the denomi-  
 493 nator correspond to the first three terms of Eq. (25).

494 Finally, using Eq. (A10), the inharmonicity be-  
 495 tween the first two resonance frequencies can be cal-  
 496 culated from the ratio of the two frequencies:

$$\frac{f_2}{2f_1} = \frac{\ell + x_1 - z_1}{\ell + x_1 - z_2} = \frac{45 - \pi^4 \beta^5}{45 - 16\pi^4 \beta^5}. \quad (27)$$

497 This gives 8% (more than a semi-tone) for the short-  
 498 est length considered (0.35 m), and 1% for the longest  
 499 length (0.67 m). As a consequence, the choice of the  
 500 mouthpiece volume reduces the inharmonicity, but in-  
 501 harmonicity remains important.

## 502 5 Analytical study of the trans- 503 fer functions for the harmon- 504 ics of the playing frequency

505 In order to investigate the spectrum of the acous-  
 506 tic quantities, we need to calculate their values at  
 507 the harmonics of the playing frequency. The anti-  
 508 formants of the input pressure and flow rate corre-  
 509 spond to the frequencies of the minima and maxima  
 510 of the input impedance sampled at the harmonics of  
 511 the playing frequency.

### 512 5.1 Input impedance extrema for the 513 harmonics of the playing fre- 514 quency

515 When the length correction for the playing frequency  
 516 is ignored (or independent of the length  $\ell$ ), it was  
 517 noticed in [23] that, for the harmonics of the play-  
 518 ing frequency, the frequencies of some extrema of the  
 519 sampled input impedance are independent of the cone  
 520 length, i.e., of the note. Indeed, for the harmonics  
 521 of the playing frequency,  $f = nc/2(\ell + x_1 - z)$ , i.e.,

522  $k\ell = n\pi - k(x_1 - z)$ , the following equation can be  
 523 written as:

$$\cot(k\ell) = -\cot(k(x_1 - z)). \quad (28)$$

524 If  $z$  is independent of the length  $\ell$ , the latter dis-  
 525 appears in the expressions of the zeros of the transfer  
 526 functions. The values of the impedance for the har-  
 527 monics of the playing frequency are located on the  
 528 following curve:

$$Z = \frac{\rho c}{S_1} \frac{j \sin(k(x_1 - z))}{- \cos(k(x_1 - z)) + \sin(k(x_1 - z))H(kx_1)}. \quad (29)$$

529 where  $H(kx_1) = [1/(kx_1) - kx_1/3]$ . Therefore the  
 530 extrema of this expression do not depend on  $\ell$  and are  
 531 common to all notes. They correspond to the zeros  
 532 of the following equations, derived from Eqs. (21 and  
 533 22) with Eq. (28):

$$\tan(k(x_1 - z)) = 0 \quad (30)$$

$$\cot(k(x_1 - z)) = 1/kx_1 - kx_1/3. \quad (31)$$

534 The first equation gives the frequencies of the  
 535 impedance minima, while the second gives those of  
 536 the impedance maxima.

537 What happens if  $z$  is slowly varying with the length  
 538  $\ell$ ? The corresponding extrema vary little with  $\ell$ .  
 539 Figure 5 shows the input impedance modulus for the  
 540 harmonics of the playing frequency. The results for 25  
 541 values of the length are superimposed. A dotted line  
 542 shows an example of input impedance for a given note.  
 543 The length correction  $-z$ , as numerically calculated  
 544 in Section 4, slightly varies with the length  $\ell$ , so do  
 545 the values of the frequencies of the extrema. They are  
 546 included in a small range. This enlarges the formants  
 547 and anti-formants of the impedance curve sampled at  
 548 the harmonics of the playing frequencies.

549 In the next subsections the values of the zeros of the  
 550 transfer functions, i.e., the solutions of Eqs. (30) and  
 551 (31), are investigated. The zeros of Eq. (30) give the  
 552 anti-formants of the input pressure, while the zeros of  
 553 Eq. (31) give the anti-formants of the flow rate.

In order to obtain more general results, we extend  
 the model of the resonator. The mouthpiece is as-  
 sumed to remain lumped and lossless, with a volume  
 equal to  $\eta S_1 x_1/3$  (for  $\eta = 1$ , it is that of the missing  
 cone), but an acoustic mass  $M_m = \sigma \rho x_1/S_1$  is added  
 (for  $\sigma = 1$ , this is that of a cylinder of length  $x_1$  and  
 cross section area  $S_1$ ). Adding an acoustic mass does  
 not make the calculation of the resonator more com-  
 plicated, while the complete computation algorithm  
 for the oscillations should be more complicated. It  
 is the reason why the model extension is limited to  
 this section. Eqs. (30) and (31) are replaced by the  
 following:

$$-1/(\sigma kx_1) = -\cot(k(x_1 - z)) + 1/(kx_1) \quad (32)$$

$$kx_1\eta/3 = -\cot(k(x_1 - z)) + 1/(kx_1). \quad (33)$$



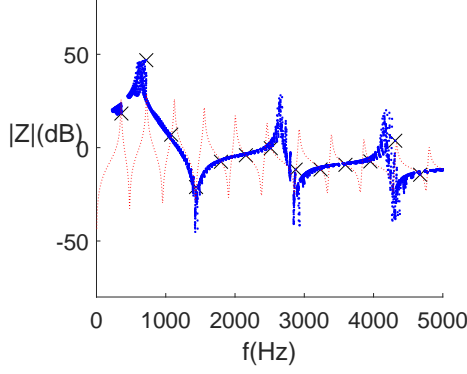


Figure 5: Values of the input impedance for the harmonics of 25 fundamental frequencies included in the first register of a soprano saxophone (thick points, blue online), corresponding to 25 values of the truncated cone length  $\ell$ . The impedance is calculated from Eq. (8), and plotted in dB:  $20\log(|ZS_1/\rho c|)$ . The frequency is in Hz. The calculation of the playing fundamental frequencies uses the results presented in Fig. 4 for  $\gamma = 0.4$ ;  $\zeta = 0.65$ . In order to exhibit an example, the results for one length is indicated by a cross 'X' for  $\ell=0.352$  m, and the complete impedance curve for this length is drawn by a thin line (red online).

554 These equations correspond to the equality of the  
 555 admittances (divided by the factor  $j\rho c/S_1$ ), when pro-  
 556 jected on the two sides of the junction. The output  
 557 of the mouthpiece is on the left-hand side, while the  
 558 input of the truncated cone is on the right-hand side.  
 559 For Eq. (32), the input impedance of the mouthpiece  
 560 vanishes, i.e., it goes through a minimum, while for Eq.  
 561 (33), it is infinite, i.e., it goes through a maximum.  
 562 Using Eq. (28), the parameter  $\ell$  has been substituted  
 563 by the parameter  $z$ . In the following subsections, ap-  
 564 proximated solutions of Eqs. (32) and (33) are sought  
 565 with respect to  $z$  and  $\sigma$  or  $\eta$  as:

$$kx_1 = n\pi(1 + \varepsilon), \quad (34)$$

566 where  $\varepsilon$  is a small unknown. Therefore

$$\tan(k(x_1 - z)) \simeq n\pi(\varepsilon - z/x_1) \quad (35)$$

567 after expanding the tangent function to the first order  
 568 in  $\varepsilon$  and  $z/x_1$ .

## 5.2 Frequencies of the input flow rate anti-formants vs the playing frequencies

572 The frequencies of the flow rate anti-formants (which  
 573 correspond to the maxima of the sampled impedance)  
 574 are first investigated by using Eqs. (33) and (35). At  
 575 the first order in  $\varepsilon$  and  $z/x_1$ , straightforward algebra

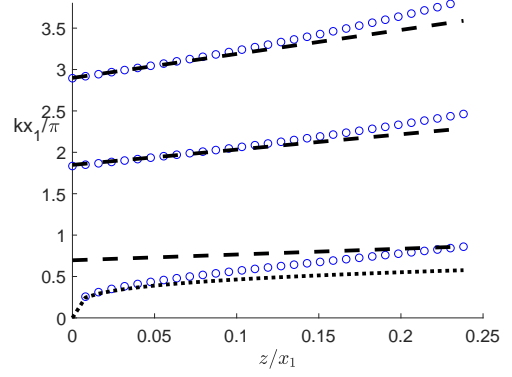


Figure 6: Frequency of the impedance maxima for the harmonics of the playing frequency with respect to the length  $z$ .  $\eta = 1$ . Circles: numerical results of Eq. (33) (blue online); dashed lines: Eqs. (37), for  $n = 1, 2, 3$ ; dotted line: Eq. (38).

leads to the following result: 576

$$\varepsilon = -\frac{1}{\alpha_n} + \frac{z}{x_1} \left[ 1 - \frac{1}{\alpha_n} \right], \text{ with } \alpha_n = \frac{\eta}{3} n^2 \pi^2. \quad (36)$$

Thus 577

$$kx_1 = n\pi \left[ 1 - \frac{1}{\alpha_n} \right] \left[ 1 + \frac{z}{x_1} \right]. \quad (37)$$

578 Figure 6 shows the comparison between Eq. (37)  
 579 and the exact solutions of Eq. (33). The agreement of  
 580 Eq. (37) with the exact result is satisfactory, except  
 581 for  $n = 1$ . For this value it is found that when  $z/x_1$   
 582 is small, the quantity  $\varepsilon$  is not small (equal to  $-1/3$ ).  
 583 For  $n = 1$  and small  $z/x_1$  the formula (37) needs to  
 584 be replaced by the solution of Eq. (A10) of Appendix  
 585 A, as follows: 586

$$kx_1 = (45z/x_1)^{1/4} \quad (38)$$

587 if  $\eta = 1$ . Fig. 6 shows the case  $\eta = 1$ . Similar  
 588 behaviour is found when the mouthpiece volume is  
 589 different ( $\eta \neq 1$ ). Eq. (38) shows that for small  $z$ ,  
 590 there is a great variation of the frequency of the first  
 591 formant. The variation of the other solutions with  $z$   
 592 (for  $n = 2, 3$ ) in Eq. (37) is significant, but narrower.  
 593 As an example, for the case in study and  $n = 2$ , 20%  
 594 is a typical variation. This is related to the width of  
 595 formants.

## 5.3 Frequencies of the input pressure anti-formants vs the playing frequencies

599 The frequencies of the pressure anti-formants (which  
 600 correspond to the minima of the sampled impedance)  
 601 are obtained by using Eqs. (33) and (35). The result  
 602 is

$$kx_1 = n\pi(1 + \sigma)(1 + z/x_1). \quad (39)$$

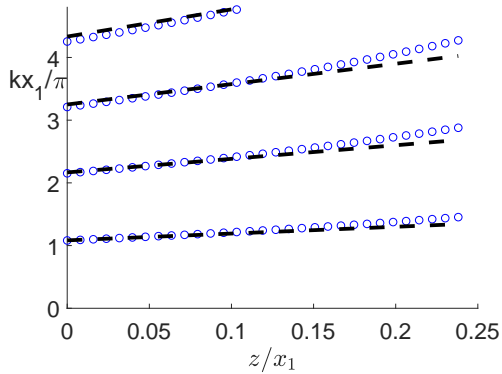


Figure 7: Frequency of the impedance minima for the harmonics of the playing frequency with respect to the length  $z$ . Circles: numerical results (blue online); dashed lines: Eq. (39) for  $\sigma = 1/12$ .

603 These frequencies are also slightly higher than the  
604 values  $n\pi$ , which would be the values for the ideal  
605 Helmholtz motion. Moreover they vary significantly  
606 with  $z$ , i.e., with the playing frequency of the note  
607 played. The order of magnitude of the variation is  
608 the same as that for the flow rate. Fig. 7 compares  
609 this formula with the exact solutions of Eq. (30). The  
610 agreement is sufficient for an estimation of the influ-  
611 ence of the pair of parameters  $(z/x_1, \sigma)$ . The value  
612 of the mouthpiece parameters have been chosen as  
613 follows: the mouthpiece is assumed to be cylindrical,  
614 with a cross section area  $S_m = 2S_1$ , and a volume  
615  $S_m \ell_m$  is equal to that of the missing cone length ( $\ell_m$   
616 is the mouthpiece length)

$$\sigma = \frac{S_1 \ell_m}{S_m x_1} = \frac{1}{3} \left( \frac{S_1}{S_m} \right)^2 = \frac{1}{12}. \quad (40)$$

617 For a cylindrical saxophone, the common minimum  
618 when  $x_1$  is constant and  $\ell$  varies, is given by  $kx_1 = n\pi$ ,  
619 i.e.,  $\sin(kx_1) = 0$ . Because  $z = 0$  for a cylindrical  
620 saxophone, this is in accordance with Eq. (39), if  
621 the acoustic mass of the small part of the cylinder is  
622 ignored.

623 As a conclusion, the frequencies of the anti-  
624 formants of both the input pressure and the input  
625 flow rate are increasing functions of the length  $z$ . Fur-  
626 therore the frequencies of the pressure anti-formants  
627 depend in a non negligible way on the acoustic mass  
628 of the mouthpiece.

## 6 Numerical results for the spectra

### 6.1 Internal and external spectra for a given length.

633 After the study of the transfer functions, we use the  
634 numerical solving of the full RTC model, including the

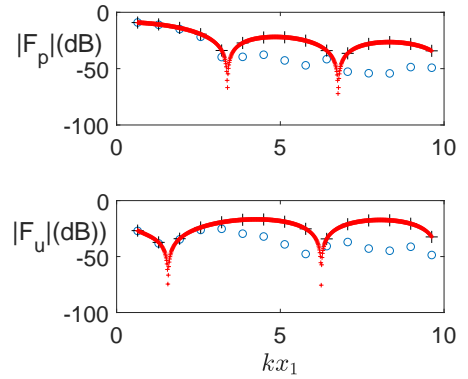


Figure 8: (top) Comparison between the input pressure  $P$  (ooo, blue online) for the harmonics of the playing frequency (275Hz) and the transfer function  $F_p$  (+++ black online).  $x_1 = 0.126\text{m}$ ,  $\ell = 0.4$ ,  $m\gamma = 0.4$ ,  $\zeta = 0.65$ . (bottom) Comparison between the input flow rate  $U$  (ooo) for the harmonics of the playing frequency and the transfer function  $F_u$  (+++) (. The small crosses (red online) represent the transfer functions for a continuous variation of the frequency. Plot in logarithmic scale:  $20\log(|F_p|)$  and  $20\log(|F_u\rho c/S_1|)$ .

excitation, and find the input pressure  $P$ , the input  
635 flow rate  $U$ , and the normalized output flow rate  $W$   
636 (see Eq. (19)), which is proportional to the external  
637 pressure. The RTC model [16] gives the input quan-  
638 tities, and the value of the outgoing pressure wave,  
639 which is denoted  $P_2^+ = P^+(x_2)$  (see Eq. (3)). The  
640 output flow rate can be derived as follows:  
641

$$U_2 = 2 \frac{S_2}{\rho c} P_2^+, \text{ therefore } W = 2P_1^+ \frac{kx_1}{j\gamma}. \quad (41)$$

642 The chosen model is the simplest ( $\eta = 1$ ;  $\sigma = 0$ , see  
643 Eqs. (32, 33)). Fig. 8 (top) shows the comparison  
644 between the spectrum modulus of the transfer func-  
645 tion  $F_p$  (Eq. (21)) and that of the input pressure  
646 signal  $P$ . For a cylindrical saxophone, because  $W$   
647 is unity (see Section 3.2), the two spectra would be  
648 identical. It appears that the effect of the cone trun-  
649 cation and the mouthpiece are significant, except for  
650 the first harmonics. The output flow rate cannot be  
651 infinite, therefore the zeros of the transfer function  
652  $F_p$  are zeros of the input pressure signal. For a bet-  
653 ter comparison between  $P$  and  $F_p$ , we complete the  
654 transfer function at intermediate frequencies, by us-  
655 ing Eq. (28), i.e., by replacing  $k\ell$  by  $-k(x_1 - z)$   
656 in the expressions (21). The values at the harmonics  
657 of the playing frequency are located on this curve.

658 The bottom of the figure allows similar observations  
659 when comparing the transfer function  $F_u$  (Eq. (22))  
660 and the spectrum of the input flow rate  $U$ .

661 Fig. 9 shows the normalized output flow rate  $W$ .  
662 For a cylindrical saxophone, it would be equal to unity  
663 (i.e., the logarithm would vanish). In order to check

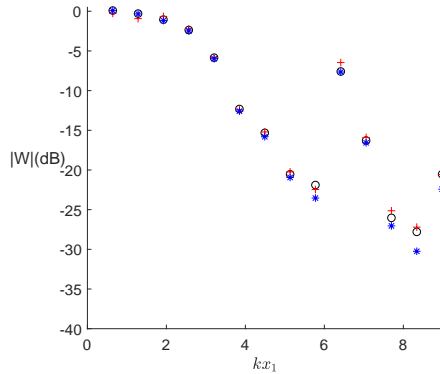


Figure 9: Normalized output flow rate  $|W|$ . Eq. (19) is computed in 3 ways: direct computation of the spectrum from the time-domain (\*\* blue online),  $|P/F_p|$  (ooo black online),  $|U/F_U|$  (+++ red online). dB is  $20\log(|W|)$  (for a cylindrical saxophone,  $20\log(|W|)$  vanishes).  $x_1 = 0.126\text{m}$ ,  $\ell = 0.4, m$   $\gamma = 0.4$ ,  $\zeta = 0.65$ .

664 the consistency of the results, the computation of  
 665  $W$  was done by using the direct result of the time-  
 666 domain calculation, then the computation of the ra-  
 667 tios  $|P/F_p|$ ,  $|U/F_U|$ . The (small) discrepancies can  
 668 be due to numerical error in the determination of the  
 669 playing frequency, or in the calculation of the spectra.

670 It appears that for higher harmonics, the flow rate  
 671 is much lower than that of the Helmholtz motion. A  
 672 maximum appears at  $kx_1 = 6.2$ . For a soprano saxo-  
 673 phone, this corresponds to a frequency equal to 2700  
 674 Hz. Benade and Lutgen [29] found what they called  
 675 “notches” in the external pressure signals, when aver-  
 676 aged over the room of the recording. A precise com-  
 677 parison with our results seems to be difficult, because  
 678 of the simplicity of our model. A comparison with a  
 679 more complete model should be useful.

## 6.2 Anti-formants in the internal spec- 681 trum

682 The transfer functions (Eq. (21, 22)) are calculated  
 683 for 32 values of the length  $\ell$  and for the harmonics  
 684 of the playing frequencies. The curves are superim-  
 685 posed in Fig. 10. Strong minima appear, therefore  
 686 anti-formants can be expected in the spectra of the  
 687 internal pressure and the internal flow rate. The fig-  
 688 ure 10 shows that despite the variation of the length  
 689 correction  $-z$  with the note played, the frequencies of  
 690 the minima and maxima vary little with the note, in  
 691 accordance with the results of Sect. 5. The central  
 692 values of the minima depend on a unique parameter,  
 693  $x_1$ . The first ones are located at:  $kx_1 = 3.4; 6.7; 10.1$   
 694 for  $F_p$  and  $1.6; 6.2; 9.9$  for  $F_u$ .

695 Fig. 11 is obtained with the RTC model. It con-  
 696 firms that anti-formants exist for the two input quan-  
 697 tities, at the position of the minima of the transfer

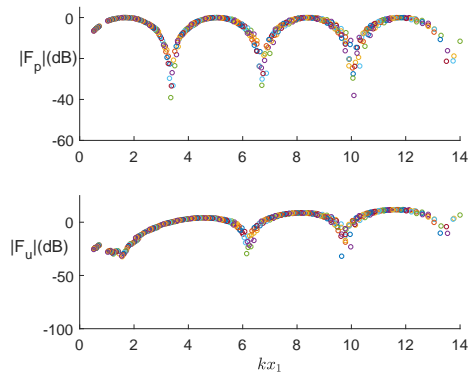


Figure 10: Transfer functions  $|F_p|$  and  $|F_U|$  for 32 values of the the length  $\ell$ . Plot in dB  $20\log(|F_p|)$  and  $20\log(|F_u\rho c/S_1|)$ .  $x_1 = 0.126\text{m}$ ,  $\ell = 0.33\text{m}$  to  $0.64\text{m}$   $\gamma = 0.4$ ,  $\zeta = 0.65$ .

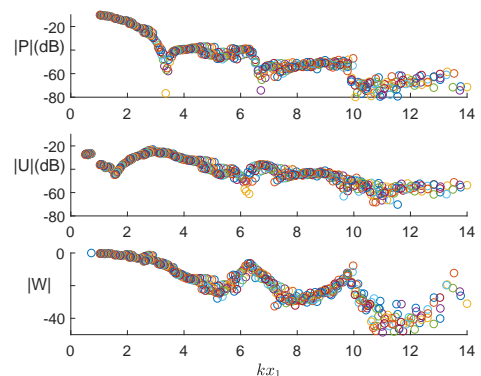


Figure 11: Input pressure  $P$ , input flow rate  $U$ , normalized output flow rate  $W$  for 32 values of the length  $\ell$  (in dB:  $20\log(|P|)$ ,  $20\log(|U\rho c/S_1|)$ ,  $20\log(|W|)$ ).  $x_1 = 0.126\text{m}$ ,  $\ell = 0.33\text{m}$  to  $0.64\text{m}$   $\gamma = 0.4$ ,  $\zeta = 0.65$ .

698 functions. For a truncated cone, their width depends  
 699 on the variation of the length correction with the cone  
 700 length. We checked that the influence of the excita-  
 701 tion parameters is weak.

702 What happens for the external spectrum, propor-  
 703 tional to that of  $W$ ? Formants seem to exist near  
 704  $kx_1 = 6.2$  and  $10$ , and maybe anti-formants near  
 705  $kx_1 = 5, 8$  and  $11$ . There is a significant difference  
 706 with the anti-formants of the input quantities: we do  
 707 not know the relationship with the transfer functions.  
 708 It could be supposed that they depend mainly on the  
 709 excitation, but this is not the case. Changing the val-  
 710 ues of the excitation parameters does not modify the  
 711 general shape of the Figure 11, including the values of  
 712 the extrema. Moreover the dependence on the mouth-  
 713 piece volume appears to be slight. The determination  
 714 of the correlation between the resonator model and  
 715 the formants and anti-formants remains a topic to be  
 716 investigated, but probably with a much more com-  
 717 plete model. This will be discussed now in the light

718 of experimental results.

## 719 7 Experimental results for the 720 mouthpiece pressure, com- 721 parison with the RTC model

722 Decreasing chromatic scales (16 notes of the first reg-  
723 ister) were played by a saxophonist for a soprano sax-  
724 ophone Selmer Mark VI, an alto saxophone Buffet-  
725 Crampon Senzo, and a baritone saxophone (Yanagi-  
726 sawa B-901). A microphone Endevco 8507-C2 is lo-  
727 cated within the mouthpiece. The Fourier analysis  
728 (FT) is done on one period, choosing a portion of each  
729 note where the pitch is rather stable.

730 Figure 12 shows the results for the internal pres-  
731 sure. The similarity of the results for the three saxo-  
732 phones, when scaled by the length  $x_1$ , is remarkable  
733 up to  $kx_1 \simeq 6$ . This value corresponds to 2580 Hz,  
734 1650 Hz, and 1080 Hz, respectively. This confirms the  
735 essential significance of the length of the missing cone  
736 at low frequencies. Using a first order filter, we com-  
737 pute a smoothed value for the harmonics of different  
738 notes. These experimental results can be compared  
739 to the numerical results of Figure 11. The amplitudes  
740 of the experimental and theoretical results seem to be  
741 rather similar. However this direct comparison is not  
742 relevant, because the amplitudes depend on the exci-  
743 tation parameters, which were not measured for the  
744 experiment: a mezzo forte note was played with each  
745 instrument, without specific constraint for the musi-  
746 cian. However the amplitude variation from lower to  
747 higher frequencies can be compared for the three in-  
748 struments.

749 The frequencies of the minima (given by dotted ver-  
750 tical lines) are very similar for the three measured sax-  
751 ophones. However the frequencies given by the model  
752 are higher than the experimental ones. A reason can  
753 be the influence of the existence of taper variation, or  
754 that of the acoustic mass of the mouthpiece, because  
755 it is in series with the input impedance of the trun-  
756 cated cone. For simplicity, the mass is ignored in the  
757 present model, because taking the mass into account  
758 would require a very different discretized oscillation  
759 model. However, for  $\sigma$  close to 0.1, Eq. (39) gives  
760 a correct order of magnitude of the necessary correc-  
761 tion for the first frequency of minimum. Obviously,  
762 at higher frequencies, the assumption that the mouth-  
763 piece is smaller than the wavelength is questionable  
764 as well. We checked that the excitation parameters  
765 play a weak role on these frequency values.

766 An attempt to measure the external pressure was  
767 done, with a microphone close to the first open tone-  
768 hole. However, as it is known (see e.g. [5, 29, 30, 31]),  
769 the pressure spectrum strongly depends on the loca-  
770 tion of the microphone. Above cutoff (for a discussion  
771 about the definition of the cutoff frequencies due to  
772 toneholes, see Ref. [32]), the external pressure field

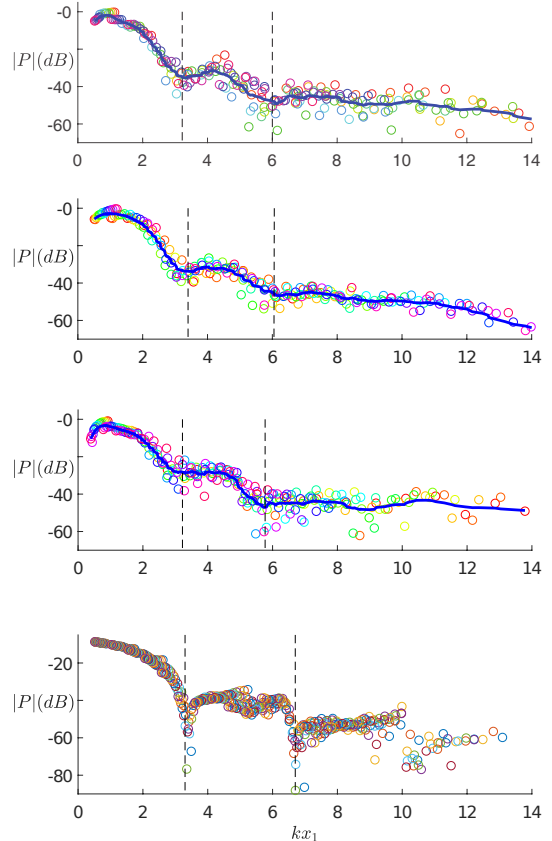


Figure 12: Mouthpiece pressure. From top to bot-  
tom: experimental results for a decreasing chromatic  
scale played on a soprano saxophone ( $x_1 = .126\text{m}$ ), an  
alto saxophone ( $x_1 = 0.196\text{m}$ ) and on a baritone sax-  
ophone ( $x_1 = 0.301\text{m}$ ) The abscissa is  $kx_1$  for the dif-  
ferent saxophones, with different  $x_1$ . Bottom: numer-  
ical results given by Fig. 11. Plot in dB:  $20\log(|P|)$ .  
Solid, line (blue online): smoothed value of the har-  
monics.

773 is the result of complicated interferences, and is very  
 774 different from the one of a monopole. For a soprano  
 775 saxophone, the cutoff can be evaluated at 1200Hz  
 776 ( $kx_1 \simeq 2.8$ ): . Moreover at this frequency the ra-  
 777 diation by the bell is not that of a monopole ( $kR_2$  is  
 778 close to 1.5). Notice that there are bends in baritone  
 779 saxophones, therefore the interference pattern is nec-  
 780 essarily different from that of the (straight) soprano  
 781 saxophone.

782 These reasons are sufficient to explain why our pre-  
 783 liminary results for the soprano and baritone saxo-  
 784 phones are very different. In Ref. [29], the authors  
 785 found that the general shapes of the external spectra  
 786 can be approximated by two straight lines, crossing  
 787 at 618 Hz for an tenor saxophone, and 837 Hz for an  
 788 alto saxophone. The first line was increasing, while  
 789 the second was decreasing. The major interest of the  
 790 approach of these authors was the measurement of an  
 791 average pressure in a room.

792 Concerning the model, it appears that the simple  
 793 theoretical model is not able to give any prediction of  
 794 the external spectrum. The first reason lies in the ig-  
 795 norance of the tonehole effects. Moreover many other  
 796 phenomena intervene: boundary layer losses, radi-  
 797 ation, reed dynamics, etc. Therefore complete study  
 798 remains to be carried out, and is out of the scope of  
 799 the present paper.

## 800 8 Conclusion

801 Conclusions can be drawn for the pressure spectrum  
 802 in the mouthpiece:

- 803 • Anti-formants exist in the spectra of the mouth-  
 804 piece pressure and input flow rate, and their  
 805 frequencies are mainly related to the resonator.  
 806 The values of their frequencies are related to the  
 807 length of the missing cone. Formants exist as  
 808 well. Their effect is less strong, but their exis-  
 809 tence can be regarded as a consequence of that  
 810 of anti-formants.
- 811 • Concerning the spectra of different instruments  
 812 of the saxophone family, they appear to be very  
 813 similar, taken into account the scaling of the  
 814 missing cone length  $x_1$ .
- 815 • The frequencies of the anti-formants are close  
 816 to the natural frequencies of the missing cone  
 817 length, but slightly higher. This is not in con-  
 818 tradiction with the hypothesis that the product  
 819  $kx_1$ , i.e. the ratio of the missing cone length to  
 820 the wavelength, can be regarded as a small quan-  
 821 tity for these frequencies, but the explanation is  
 822 not straightforward: it is related to the consider-  
 823 ation of the *sampling* of the input impedance at  
 824 the harmonics of the playing frequency. This is  
 825 a major difference with a cylindrical saxophone,

826 for which the harmonicity of the resonance fre-  
 827 quencies is perfect, and the playing frequency is  
 828 equal to that of the first impedance peak (for the  
 829 simplest model).

- 830 • In other words, the difference between the inhar-  
 831 monicity of the resonator and the harmonicity of  
 832 the spectrum in the periodic signals explain why  
 833 minima exist in the input pressure and in the in-  
 834 put flow rate.
- 835 • Furthermore inharmonicity of a conical instru-  
 836 ment implies a variation of the negative length  
 837 correction, denoted  $-z$  in the present paper,  
 838 when the length of the truncated cone varies.  
 839 This is in particular true for the inharmonicity  
 840 due to the cone truncation. A consequence is a  
 841 small variation of the minimum pressure frequen-  
 842 cies with the length of the truncated cone, i.e.,  
 843 with the played note, and an enlargement of the  
 844 anti-formants. However, despite of this variation,  
 845 existence of anti-formants is clear.
- 846 • The simplified model of [16] allows an interesting  
 847 prediction of the waveshapes, and of the existence  
 848 of anti-formants in the spectra of the input quan-  
 849 tities. This is true at least up to  $kx_1 \simeq 7$ , i.e.,  
 850 up to a ratio of the missing cone length to the  
 851 wavelength equal to unity.
- 852 • Assuming a monopole radiation, the external  
 853 pressure diminishes with the frequency, much  
 854 more rapidly than for an ideal cylindrical saxo-  
 855 phone (see Fig. 9) . Numerical results show  
 856 that formants exist for the external spectrum and  
 857 their dependence on the excitation parameters is  
 858 weak. However their dependence on the geomet-  
 859 rical parameters remains to be understood. It  
 860 cannot be easily derived from that of the input  
 861 quantities.
- 862 • A convincing comparison with experiment re-  
 863 quires both a much more complete model and  
 864 measurements at different microphone locations  
 865 of the radiated sound.

## 866 Acknowledgements

867 We thank Sandra Ndayizamba very much for playing  
 868 the Senzo saxophone, and the Buffet-Crampon com-  
 869 pany for lending the instrument. We thank also G.  
 870 Rabau and T. Colinot for helping the preparation of  
 871 the paper. This work was done in the frameworks  
 872 of Labex MEC (ANR-10-LABX-0092) and of the  
 873 A\*MIDEX project (ANR-11-IDEX-0001-02), funded  
 874 by the French National Research Agency (ANR). It  
 875 was also supported by the SDNS-AIMV project fi-  
 876 nanced by the ANR (project ANR-09-RPDOC-022-  
 877 01), and the LabCom LIAMFI ANR project (ANR-  
 878 16-LCV2-0007-01).

## Appendix A: Approximate calculations of the playing frequency

The formula (24) can be rewritten by applying the residue calculus to the modal expansion of the input impedance (Eq. (8), see e.g. Ref. [19], p. 167):

$$Z(\omega) = \sum_m \frac{Res_m}{\omega_p - \omega_m}. \quad (\text{A1})$$

The  $\omega_m$ 's are the poles and the  $Res_m$ 's are the residues. Because the input impedance is written in the form (8), which ensures that the numerator has no pole, the residues are obtained as the ratio of the numerator to the derivative of the denominator (see [19] p. 167). Because no losses are considered, the poles are real. An approximate value of  $Z(\omega)$  at a given frequency can be found by truncating the series to one term only, which corresponds to the pole which is closest to this frequency. It is assumed that the frequency  $\omega_m$  is close to  $n\omega$ , therefore the subscript  $m$  is replaced by  $n$ . With this assumption, Eq. (24) becomes:

$$\sum_n n |P_n|^2 (n\omega_p - \omega_n) / Res_n = 0, \quad (\text{A2})$$

therefore:

$$\omega_p = \frac{\sum_n n |P_n|^2 \omega_n / Res_n}{\sum_n n^2 |P_n|^2 / Res_n}. \quad (\text{A3})$$

If all natural frequencies are harmonically related,  $\omega_n = n\omega_1$ , and  $\omega_p = \omega_1$ . Another expression can be found by defining the length corrections  $z_n$  for the different resonance frequencies, as follows:

$$k_n = \frac{\omega_n}{c} = \frac{n\pi}{\ell + x_1 - z_n} \simeq \frac{n\pi\beta}{x_1} \left( 1 + z_n \frac{\beta}{x_1} \right). \quad (\text{A4})$$

The latter expression is valid at the first order of  $z_n/(\ell + x_1)$ . Using this expression, and a similar expression for  $k_p$  derived from Eq. (23), Eq. (A2) becomes:

$$z = \frac{\sum_n z_n n^2 |P_n|^2 / Res_n}{\sum_n n^2 |P_n|^2 / Res_n}. \quad (\text{A5})$$

If the pressure spectrum is assumed to be that of the Helmholtz motion (Eq. (13)), Eq. (25) is obtained. Two calculations of the values of  $z_n$  and  $Res_n$  are used: i) an exact calculation of the resonance frequencies, which are zeros of the the input impedance (Eq. (11)), and the corresponding residues; ii) an analytical approximation of these quantities.

It is possible to slightly enlarge the hypothesis for Eq. (25). Now the volume of the mouthpiece is not

necessarily equal to that of the missing cone. We denote it  $V = \eta x_1 S_1 / 3$ . For the exact volume of the missing cone,  $\eta = 1$ . In the denominator of Eq. (8), the factor  $1/3$  is replaced by  $\eta/3$ , thus the resonances are given by:

$$\cot(k\ell) + 1/(kx_1) - \eta kx_1/3 = 0, \quad (\text{A6})$$

The poles are numerically computed as solutions of Eq. (A6). From Eq. (8), the residues are found to be:

$$Res_n^{-1} = -\frac{S_1}{j\omega\rho} \frac{\ell + x_1 + k_n^2 x_1^2 (\ell (1 - \frac{2\eta}{3} + \frac{\eta x_1}{3} - \frac{2\ell}{3} k_n^2 x_1^2) + \eta^2 \frac{\ell}{9} k_n^4 x_1^4)}{k_n^2 x_1^2}. \quad (A7)$$

924



925 where  $k_n = \omega_n/c$  are numerically computed as so-  
 926 lutions of Eq. (A6). Using Eq. (A4), the length cor-  
 927 rections of the resonance frequencies  $z_n$  are deduced.  
 928 Then Eq. (25) is directly calculated (remember that  
 929 Eq. (25) is an approximation, because the real spec-  
 930 trum of the input pressure is replaced by that of the  
 931 Helmholtz motion). Figure 4 shows that for  $\eta = 1$   
 932 Eq. (25) gives lower and upper bounds for the exact  
 933 values, when two and three terms of the series are  
 934 taken into account. When  $\eta$  is slightly different of  
 935 unity, the length correction is significantly modified,  
 936 but Eq. (25) remains satisfactory.

937 The second kind of calculation needs a further  
 938 step. A first simplification is to approximate the res-  
 939 onance frequencies by those of the Helmholtz motion  
 940 ( $k_n = n\pi\beta$ ). This is a good approximation, entail-  
 941 ing a small error (of the second order in  $z/x_1$ ). The sec-  
 942 ond simplification is based on the approximated cal-  
 943 culation of the length corrections  $z_n$ , by using a series  
 944 expansion, as follows. From the definition (A4),

$$\cot(k_n\ell) = -\cot(k_n(x_1 - z_n)). \quad (\text{A8})$$

945 Therefore Eq. (A6) can be rewritten as:

$$\cot(k_n(x_1 - z_n)) = +\frac{1}{kx_1} - \frac{\eta kx_1}{3}. \quad (\text{A9})$$

946 If the argument of the cotangent function is small,  
 947 the following expansion can be used:  $\cot(x) \simeq 1/x -$   
 948  $x/3 - x^3/45$ . At this order of the cotangent function  
 949 and at the first order in  $z_n/x_1$  (see Eq. (A4)), this  
 950 leads to the following result:

$$z_n/x_1 = \frac{k_n^2 x_1^2}{3} \left[ 1 - \eta + \frac{k_n^2 x_1^2}{3} \left( \frac{1}{5} + \eta - 1 \right) \right]. \quad (\text{A10})$$

951 The order of the expansion limits the value of  
 952  $nk_1x_1 \simeq n\pi\beta$  to approximately unity.  $\beta$  being smaller  
 953 than unity, the following calculation is limited to  
 954  $n = 3$ , and this implies the truncation of the series  
 955 in Eq. (A2). For the case  $\eta = 1$ , the final result is  
 956 found to be:

$$z \simeq x_1 \frac{\pi^4 \beta^4}{45} \frac{\sum_{n=1}^3 n^2 \sin^2(n\pi\beta)}{\sum_{n=1}^3 n^{-2} \sin^2(n\pi\beta)}. \quad (\text{A11})$$

957 We remind that the length correction is  $-z$ . This  
 958 can be rewritten as Eq. (26). Equations (A3) and  
 959 (A5) can be used for other causes of inharmonicity.  
 960 For that purpose, it could be interesting to analyse in  
 961 details all causes of inharmonicity, as did Debut [33]  
 962 for a clarinet. As an example, the inharmonicity due  
 963 to open toneholes is negative (with a positive length  
 964 correction), while that due to the cone truncation is  
 965 positive. Such an effect can be large for fork finger-  
 966 ings [34], and entails significant effect on the playing  
 967 frequency.

## References

- 968
- [1] R.A. Smith and D.M.A. Mercer, Possible causes  
 969 of woodwind tone colour, *J. of Sound Vib.* 32,  
 970 347-358 (1974) 971
- [2] W. Voigt. Research on the formant formation in  
 972 sounds of dulcians and bassoons, *Kölner Beiträge*  
 973 *zur Musikforschung*, Band 5 (in German), Gus-  
 974 tav Bosse (1975) 975
- [3] A.H. Benade, Wind instruments and music  
 976 acoustics. In *Sound generation in winds strings*  
 977 *computers*, Royal Swedish Academy of Music No.  
 978 29, 15-99 (1980). 979
- [4] F. Fransson, The source spectrum of double-reed  
 980 wood-wind instruments, Part 1. The bassoon,  
 981 *Quarterly Progress and Status Report*, Dept. for  
 982 Speech, Music and Hearing, 8, 35-37 (1967). 983
- [5] D.H. Keefe, Woodwind tone hole acoustics and  
 984 the spectrum transformation function, PhD,  
 985 Case Western Reserve University (1981) 986
- [6] J. Saneyoshi, Theory on Anti-resonance Frequen-  
 987 cies of Input Impedance of Conical Horns, --- Os-  
 988 cillation Frequencies of Wind Instruments with a  
 989 Conical Pipe (in Japanese), *Proc. of the Acous-*  
 990 *tical Society of Japan*, Autumn Meeting, 65-66  
 991 (1977) 992
- [7] A. Ya. Gokhshtein, Pressure jumps in the reflec-  
 993 tion of a wave from the end of a tube and their  
 994 effect on the pitch of sound, *Sov. Phys. Doklady*  
 995 25, 462-464 (1980). 996
- [8] J. P. Dalmont, J. Kergomard: Elementary model  
 997 and experiments for the Helmholtz motion in  
 998 conical woodwinds. *Proceedings of the Interna-*  
 999 *tional Symposium of Musical Acoustics*, Dour-  
 1000 dan, 114-120 (1995) 1001
- [9] J.-P. Dalmont, J. Gilbert, and J. Kergomard,  
 1002 Reed Instruments, from small to large amplitude  
 1003 periodic oscillations and the Helmholtz motion  
 1004 analogy, *Acustica united with Acta Acustica* 86,  
 1005 671-684 (2000). 1006
- [10] S. Ollivier, J.-P. Dalmont, and J. Kergomard,  
 1007 Idealized Models of Reed Woodwinds. Part I:  
 1008 Analogy with the Bowed String, *Acta Acustica*  
 1009 *united with Acustica*, 90, 1192-1203 (2004). 1010
- [11] S. Carral and V. Chatziioannou, Influence of the  
 1011 cone parameters on the sound of conical wood-  
 1012 wind instruments, *Proceedings of the ISMA*, 201-  
 1013 206, Le Mans, France (2014). 1014
- [12] J.-B. Doc, C. Vergez, P. Guillemain, J. Ker-  
 1015 gomard, Sound production on a “coaxial sax-  
 1016 ophone”, *J. Acoust. Soc. Am.*, 140, 3917-3924  
 1017 (2016). 1018

- 1019 [13] E.J. Irons, On the fingering of conical instru- 1070  
1020 ments. The London, Edinburgh, and Dublin 1071  
1021 Philosophical Magazine and Journal of Science, 11, 535-539, Iss. 70 (1931). 1072  
1022 1073
- 1023 [14] A.H. Benade, On woodwind instruments bores. 1074  
1024 J. Acoust. Soc. Am. 31, 137-146 (1959) 1075
- 1025 [15] C.J. Nederveen, Acoustical aspects of woodwind 1076  
1026 instruments. Northern Illinois (1983). 1077
- 1027 [16] J. Kergomard, P. Guillemain, F. Silva and S. 1078  
1028 Karkar, Idealized digital models for conical reed 1079  
1029 instruments, with focus on the internal pressure 1080  
1030 waveform. J. Acoust. Soc. Am. 139, 927-937, 1081  
1031 (2016). 1082
- 1032 [17] A. H. Benade and W. Bruce Richards, Oboe nor- 1083  
1033 mal mode adjustment via reed and staple pro- 1084  
1034 portioning, J. Acoust. Soc. Am. 73, 1794-1803 1085  
1035 (1983). 1086
- 1036 [18] J.P. Dalmont, B. Gazengel, J. Gilbert, J. Kergo- 1087  
1037 mard, Some aspects of tuning and clean intona- 1088  
1038 tion in reed instruments. Applied Acoustics 46, 1089  
1039 19-60 (1995). 1090
- 1040 [19] A. Chaigne and J. Kergomard, Acoustics of mus- 1091  
1041 ical instruments, Springer (2016). 1092
- 1042 [20] P. Guillemain, C. Vergez, D. Ferrand, A. Farcy, 1093  
1043 An Instrumented Saxophone Mouthpiece and its 1094  
1044 Use to Understand How an Experienced Musi- 1095  
1045 cian Plays. Acta Acustica united with Acustica 1096  
1046 96, 622-634 (2010). 1097
- 1047 [21] T. Wilson and G. Beavers, Operating modes of 1098  
1048 the clarinet, J. Acoust. Soc. Am. 56, 653-658  
1049 (1974).
- 1050 [22] J.P. Dalmont, B. Gazengel, J. Kergomard, Scal-  
1051 ing of reed instruments: The case of the sax-  
1052 ophone family. J. Acoust. Soc. Am. 119, 3259  
1053 (2006).
- 1054 [23] J.Kergomard, Ph. Guillemain, S. Karkar, J.P.  
1055 Dalmont, B. Gazengel, What we understand to-  
1056 day on formants in saxophone sounds? 44<sup>o</sup>  
1057 Congreso Español de Acústica, 1209-1216, Val-  
1058 ladolid (2013).
- 1059 [24] A.H. Benade, Fundamental of musical acoustics,  
1060 Oxford University Press (1976).
- 1061 [25] W. Worman: Self-sustained nonlinear oscilla-  
1062 tions of medium amplitude in clarinet likesys-  
1063 tems. Ph.D. thesis, Case Western Reserve Uni-  
1064 versity Cleveland (1971).
- 1065 [26] W. Coyle, P. Guillemain, J. Kergomard and J.P.  
1066 Dalmont. Predicting playing frequencies for clar-  
1067 inets: A comparison between numerical sim-  
1068 ulations and simplified analytical formulas, J.  
1069 Acoust. Soc. Am., 138, 2770-2781 (2015).
- [27] B. Ricaud, P. Guillemain, J. Kergomard, F. 1070  
1071 Silva, C. Vergez, Behavior of reed woodwind 1072  
1073 instruments around the oscillation threshold, 1074  
Acta Acustica united with Acustica, 95,733-743  
(2009).
- [28] X. Boutillon, Analytical investigation of the flat- 1075  
1076 tening effect—the reactive power balance rule, J. 1077  
Acoust. Soc. Am. 90, 754–763 (1991).
- [29] A.H. Benade and S. J. Lutgen, The saxophone 1078  
1079 spectrum, J. Acoust. Soc. Am. 83, 1900-1907  
(1988). 1080
- [30] J. Kergomard, Internal and external field of wind 1081  
1082 instruments (in French), Phd, University Paris 6  
(1981). 1083
- [31] A.H. Benade, From Instrument to Ear in a 1084  
1085 Room: Direct or via Recording. J. Audio Eng.  
1086 Soc. 33, 218-233 (1985). 1087
- [32] E. Moers and J. Kergomard, “On the Cutoff Fre- 1088  
1089 quency of Clarinet-Like Instruments. Geometri-  
1090 cal versus Acoustical Regularity”, Acta Acustica  
united with Acustica, 97, 984 – 996 (2011). 1091
- [33] V. Debut, J. Kergomard, and F. Laloë, “Analysis 1092  
1093 and optimisation of the tuning of the twelfths for  
a clarinet resonator,” Appl. Acoust. 66, 365–409  
(2005). 1094
- [34] C. J. Nederveen and J.-P. Dalmont, “Mode lock- 1095  
1096 ing effects on the playing frequency for fork fin-  
1097 gerings on the clarinet”, J. Acoust. Soc. Am. 131,  
689-697 (2012). 1098